6th International Symposium on Three-Dimensional Electromagnetics
Berkeley, California, March 28–30, 2017

Gauss-Newton based 3D anisotropic inversion of marine CSEM data

Ronghua. Peng[1], Xiangyun, Hu[1], Jianhui, Li[1], and Jianchao Cai[1]
[1]China University of Geosciences, Wuhan

Summary

Marine controlled source electromagnetic (CSEM) data are heavily influenced by the presence of electrical anisotropy in practice. Neglect of formation anisotropy in the interpretation of marine CSEM data may produce misleading resistivity images such as artifacts or erroneous positioning of anomalies. Here, we present an efficient 3D anisotropic inversion algorithm for marine CSEM data affected by vertical transverse isotropy (VTI). The inversion algorithm combines a direct forward solver and the Gauss-Newton approach. The direct solver used as the forward engine facilitates the reuse of the matrix factorization, which makes the solutions for multiple transmitters with little additional effort. While the Gauss-Newton approach provides balanced sensitivity to targets at different burial depths, thus producing improved resistivity models compared with gradient based inversion algorithms. Numerical experiment on synthetic marine CSEM data demonstrates that the 3D anisotropic inversion algorithm can produce reliable resistivity results in the presence of electrical anisotropy.

Keywords: marine CSEM, vertical transverse isotropy, anisotropic inversion, Gauss-Newton algorithm

Introduction

Driven by the successful applications for offshore hydrocarbon exploration, marine controlled source electromagnetic method (CSEM) has been increasingly adopted by petroleum industry as an integrated part of the exploration workflow over the past decade (e.g., Constable, 2010; MacGregor & Tomlinson, 2014). As marine CSEM surveying now moves into increasingly complex offshore geological environment, the need for quantitative interpretation of marine CSEM data in such circumstance requires developing efficient inversion tools. A significant improvement for the interpretation of practical marine CSEM data is the recognition of the effect of electrical anisotropy upon CSEM responses (Tompkins, 2005; Jing et al., 2008; Mohamad et al., 2010). It is now well recognized that sedimentary formations in the marine environment are usually characterized by strong electrical anisotropy due to sedimentation (Anderson et al., 1994; Clavaud, 2008), and the neglect of electrical anisotropy in the interpretation of practical data may cause misleading geological interpretation that undermines the power of marine CSEM technique (Hesthammer et al., 2010).

Considering the importance of formation anisotropy in the measured marine CSEM data, various 3D anisotropic inversion algorithms have been developed in order to reliably interpret the data influenced by electrical anisotropy (e.g., Newman et al., 2010; Sasaki, 2013). These anisotropic inversion algorithms commonly employ the gradient-based optimization strategies due to their minimal requirements in terms of memory storage and computational cost. However, the high sensitivity of marine CSEM data close to the receivers leads to large updates near the seafloor, making the gradient-based inversion algorithms tend to be trapped into local minima in which deep resistive targets are usually projected into shallow artifacts (Nguyun et al., 2016). Therefore, there still has been a growing effort to develop rigorous anisotropic inversion algorithms to improve the interpretation capacity of marine CSEM data.

In this work, we present a 3D anisotropic inversion approach for marine CSEM data based on Gauss-Newton (GN) optimization in combination with a direct forward solver. We assume that the resistivity model is characterized with vertical transverse isotropy (VTI), which is reasonable considering this simple form of electrical anisotropy represents the typical type of electrical anisotropy commonly encountered in the actual marine geologic settings. We first briefly introduce 3D anisotropic forward modeling using an efficient mimetic finite volume method, then describe our 3D anisotropic inversion algorithm based on GN approach, and finally illustrate the capacity of the inversion algorithm by a synthetic marine CSEM example.

The forward problem

To calculate marine CSEM responses in the frequency domain, We employ the well known scattering-field approach to mitigate the numerical singularity in the

vicinity of the transmitter, where the total field is decomposed into a primary field excited by the external current density $\mathbf{J}_s$ in a given reference model $\bar{\sigma}_0$ and an anomalous field arising from conductivity variations. Assuming a time dependence $e^{i\omega t}$ and neglecting displacement currents (i.e., quasi-stationary approximation), we solve the vector Helmholtz equation for the anomalous electric field $\mathbf{E}_s$ as follows

$$\nabla \times \mu_0^{-1} \nabla \times \mathbf{E}_s + i\omega\bar{\sigma}\mathbf{E}_s = -i\omega(\bar{\sigma} - \bar{\sigma}_0)\mathbf{E}_p \quad (1)$$

where μ_0 denotes free space magnetic permeability, ω denotes angular frequency, $\bar{\sigma}$ is the electrical conductivity tensor having different horizontal and vertical resistivities, $\mathbf{E}_p$ denotes the primary electric field for a given reference model $\bar{\sigma}_0$.

To derive a robust numerical scheme, we apply a mimetic finite volume (MFV) approximation (Hyman & Shashkov, 1999; Haber & Ruthotto, 2014) to discretize eq. (1) on a staggered grid, resulting in a large system of linear equations

$$\mathbf{A}\mathbf{E}_s = \mathbf{b}. \quad (2)$$

The sparse linear system (2) can be solved using either iterative or direct methods. Here we utilize a direct solver MUMPS (Amestoy & Puglisi, 2002) to obtain the solution to eq. (2), considering direct solvers are usually more robust than iterative ones for numerically difficult cases. Besides, for multiple source problems, the system matrix $\mathbf{A}$ is invariant at a given frequency. Therefore, the solutions for multiple source locations can be easily obtained with little additional expense by repeatedly using the same factorization.

Inverse problem formulation

It is well known that the inverse problem of CSEM data is highly ill-posed, we formulate the inverse problem using Tikhonov regularization approach (Tikhonov & Arsenin, 1977) as the minimization of the following objective functional

$$\varphi(\mathbf{m}_h, \mathbf{m}_v) = \varphi_d(\mathbf{m}_h, \mathbf{m}_v) + \beta\varphi_m(\mathbf{m}_h, \mathbf{m}_v) \quad (3)$$

where $\mathbf{m}_h$ and $\mathbf{m}_v$ are the horizontal and vertical model vectors, respectively. They are both parameterized as $\ln(\sigma)$ to enforce a positivity constraint on model parameters. β is the Tikhonov regularization parameter that controls the weighting between the data misfit term φ_d and the model regularization term φ_m. The data misfit φ_d measures the discrepancy between the observed and the predicated data, defining as

$$\varphi_d(\mathbf{m}_h, \mathbf{m}_v) = \frac{1}{2}\|\mathbf{W}_d[\mathbf{F}(\mathbf{m}_h, \mathbf{m}_v) - \mathbf{d}_{obs}]\|^2 \quad (4)$$

where $\mathbf{F}$ is the anisotropic forward modeling functional, $\mathbf{d}_{obs}$ is the observed marine CSEM data vector consisting of the real and imaginary parts of the measured electric or magnetic fields, $\mathbf{W}_d$ is the data weighting matrix characterizing data measurement uncertainties. While the model regularization term that stabilizes the ill-posed inverse problem is defined as

$$\varphi_m(\mathbf{m}_h, \mathbf{m}_v) = \frac{1}{2}\lambda_h\|\mathbf{W}_m\mathbf{m}_h\|^2 + \frac{1}{2}\lambda_v\|\mathbf{W}_m\mathbf{m}_v\|^2 \quad (5)$$

where $\mathbf{W}_m$ is the roughness matrix defined as a first order finite difference operator, the parameters λ_h and λ_v control the roughness of the horizontal and vertical resistivity models, respectively.

Due to the non-linearity of the inverse problem, we need to iteratively solve the optimization problem eq. (3) to obtain the optimal estimate of the anisotropic conductivity model that fits the observed data. Here we employ the Gauss-Newton algorithm in which the model perturbation $\delta\mathbf{m} = [\delta\mathbf{m}_h, \delta\mathbf{m}_v]^T$ at each iteration is obtained by

$$(\mathbf{J}^H\mathbf{J})\delta\mathbf{m} = -\mathbf{g} \quad (6)$$

where H denotes the complex conjugate operator, the sensitivity matrix $\mathbf{J}$, and the gradient $\mathbf{g}$ are, respectively, defined as

$$\mathbf{J} = \begin{bmatrix} \mathbf{W}_d\mathbf{J}_h & \mathbf{W}_d\mathbf{J}_v \\ \sqrt{\lambda_h}\mathbf{W}_m & \mathbf{0} \\ \mathbf{0} & \sqrt{\lambda_v}\mathbf{W}_m \end{bmatrix}, \mathbf{g} = \mathbf{J}^H \begin{bmatrix} \mathbf{W}_d\Delta\mathbf{d} \\ \sqrt{\lambda_h}\mathbf{W}_m\mathbf{m}_h \\ \sqrt{\lambda_v}\mathbf{W}_m\mathbf{m}_v \end{bmatrix} \quad (7)$$

where $\mathbf{J}_h$ and $\mathbf{J}_v$ denote data sensitivity matrix with respect to the horizontal and vertical resistivities, respectively, $\Delta\mathbf{d}$ denotes the difference between the predicted and observed data.

The sensitivity matrix $\mathbf{J}$ plays a central role for the inversion of CSEM data. For CSEM methods, the sensitivity of the electric field with respect to arbitrary model parameter σ_k within a spatial domain Ω is given by

$$\frac{\partial E}{\sigma_k} = \int_\Omega \mathbf{E} \cdot \tilde{\mathbf{E}} dv \quad (8)$$

where $\mathbf{E}$ is the actual electric fields due to the transmitter, and $\tilde{\mathbf{E}}$ is the auxiliary electric fields excited by the fictitious source at the corresponding receiver (McGillivray et al., 1994). For CSEM methods, the electric fields due to an electric dipole source are exponentially attenuated with the distance from the source, which suggests that the data sensitivity with respect to the deep target is much smaller than the shallow one according to eq. (8). For gradient-based

algorithms, the huge data sensitivity difference between objects at different burial depths often leads to undesirable inversion results such as oscillatory near surface variations (Newman et al., 2010) and shallower recovered anomalies than actual ones (Brown et al., 2012). In contrast, the Gauss-Newton algorithm usually offers much better sensitivity balancing by preconditioning the gradient using the Hessian in the search of model perturbation according to eq. (6), thus producing more favorable inversion results (Nguyun et al., 2016).

Synthetic example

We consider a synthetic marine model modified from 3D SEG/EDGE salt dome model (Aminzadeh et al., 1997) to test the 3D anisotropic inversion algorithm. The model shown in Figure 1 consists of 1 km water volume with a resistivity of 0.3 ohm-m and an anisotropic salt dome target embedded in an isotropic host layer with a resistivity of 1 ohm-m, the salt dome target is characterized by VTI medium with a horizontal and vertical resistivity of 10 ohm-m and 100 ohm-m, respectively. The data acquisition geometry shown in Figure 2 comprises 12 orthogonal surveying lines with 1 km spacing and 36 receivers uniformly deployed on the seafloor with 1 km separation between them. A horizontal electrical dipole (HED) towed 50 m above the seafloor sends EM signals at 400 m intervals moving along each surveying line at the operating frequency of 0.25 Hz. Both inline and offline horizontal E_x and E_y electric fields are used for inversion. Prior to inversion, the simulated data were contaminated with five percent Gaussian noise, and data with amplitudes below 5×10^{-15} V/m were discarded.

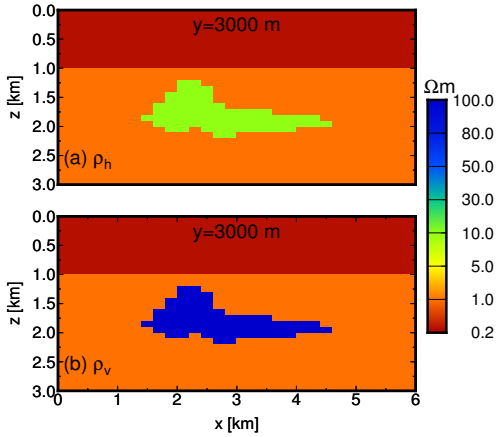

Figure 1: Cross section of 3D anisotropic salt dome model. (a) ρ_h, (b) ρ_v.

Figure 3 shows vertical cross sections of horizontal and vertical resistivity models recovered from 3D anisotropic inversion. From the horizontal resistivity image, it shows that the thick zones of the salt dome are well defined whereas the thin zones are poorly recovered, which is consistent with previous findings that marine CSEM responses produce little sensitivity to the horizontal resistivity of thin resistive target. Instead, low resistivity artifacts appear below thin zones of the target. In contrast, The resistive salt dome is clearly reconstructed at the correct depths in the vertical resistivity image.

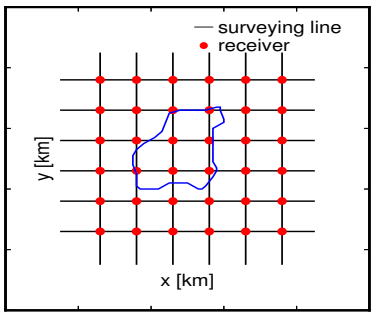

Figure 2: Sketch of data acquisition geometry used to generate marine CSEM data.

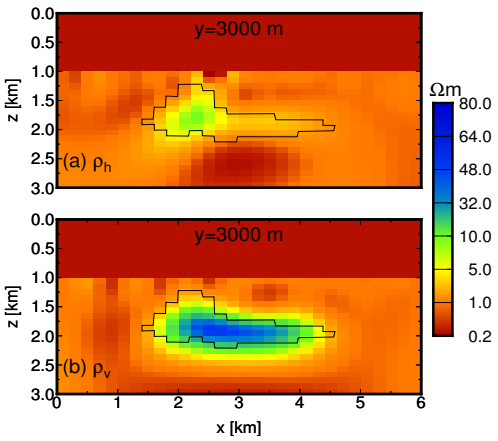

Figure 3: Cross section of recovered model from anisotropic inversion. (a) ρ_h, (b) ρ_v, anisotropic target is outlined in black.

Figure 4 shows the anisotropic ratio of vertical to horizontal resistivity obtained from 3D anisotropic inversion. An enhanced resistivity domain away from isotropy corresponding to the anisotropic salt dome structure is clearly shown.

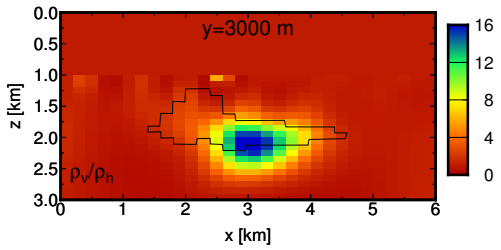

Figure 4: Cross section of anisotropic ratio of vertical (ρ_v) to horizontal (ρ_h) resistivity obtained from anisotropic inversion.

Conclusions

The presence of electrical anisotropy produces significant influence on marine CSEM responses. Failure to incorporate the electrical anisotropy may lead to misleading interpretation. We have developed a 3D anisotropic inversion algorithm for marine CSEM data based on Gauss-Newton optimization coupled with a direct forward solver. The synthetic numerical experiment clearly demonstrates that 3D anisotropic inversion algorithm can produce reliable resistivity models in the presence of electrical anisotropy from marine CSEM data, thus improving the interpretation capacity of marine CSEM data.

Acknowledgements

We appreciate the financial support from National Science Foundation of China (NO. 41274077, 41474055) and National Basic Research Program of China (NO. 2013CB733200).

REFERENCES

Amestoy, P. R., & Puglisi, C. (2002). An unsymmetrized multifrontal LU factorization. *SIAM Journal on Matrix Analysis and Applications*, *24*(2), 553-569.

Aminzadeh, F., Brac, J., & Kunz, T. (1997). 3D salt and overthrust models. *SEG*.

Anderson, B., Bryant, I., Luling, M., Spies, B., & Helbig, K. (1994). Oilfield anisotropy: Its origins and electrical characteristics. *Oilfield Review*, *6*(4), 48-56.

Brown, V., Hoversten, M., Key, K., & Chen, J. (2012). Resolution of reservoir scale electrical anisotropy from marine CSEM data. *Geophysics*, *77*(2), E147-E158.

Clavaud, J. B. (2008). Intrinsic electrical anisotropy of shale: The effect of compaction. *Petrophysics*, *49*(03).

Constable, S. (2010). Ten years of marine CSEM for hydrocarbon exploration. *Geophysics*, *75*(5), 75A67-75A81.

Haber, E., & Ruthotto, L. (2014). A multiscale finite volume method for maxwell's equations at low frequencies. *Geophysical Journal International*, *199*(2), 1268-1277.

Hesthammer, J., Stefatos, A., Boulaenko, M., Fanavoll, S., & Danielsen, J. (2010). CSEM performance in light of well results. *The Leading Edge*, *29*(1), 34-41.

Hyman, J. M., & Shashkov, M. (1999). Mimetic discretizations for Maxwell's equations. *Journal of Computational Physics*, *151*(2), 881-909.

Jing, C., Green, K., & Willen, D. (2008). CSEM inversion: Impact of anisotropy, data coverage, and initial models. In *SEG technical program expanded.* Society of Exploration Geophysicists.

MacGregor, L., & Tomlinson, J. (2014). Marine controlled-source electromagnetic methods in the hydrocarbon industry: A tutorial on method and practice. *Interpretation*, *2*(3), SH13-SH32.

McGillivray, P., Oldenburg, D., Ellis, R., & Habashy, T. (1994). Calculation of sensitivities for the frequency-domain electromagnetic problem. *Geophysical Journal International*, *116*(1), 1-4.

Mohamad, S. A., Lorenz, L., Hoong, L. T., Wei, T. K., Chandola, S. K., Saadah, N., & Nazihah, F. (2010). A practical example why anisotropy matters: A CSEM case study from south east asia. In *SEG technical program expanded.* Society of Exploration Geophysicists.

Newman, G. A., Commer, M., & Carazzone, J. J. (2010). Imaging CSEM data in the presence of electrical anisotropy. *Geophysics*, *75*(2), F51-F61.

Nguyun, A. K., Nordskag, J. I., & Wiik, T. (2016). Comparing large scale 3D Gauss-Newton and BFGS CSEM inversions. In *SEG technical program expanded.* Society of Exploration Geophysicists.

Sasaki, Y. (2013). Resolution of shallow and deep marine CSEM data inferred from anisotropic 3d inversion. In *SEG technical program expanded.* Society of Exploration Geophysicists.

Tikhonov, A. N., & Arsenin, V. (1977). *Solutions of ill-posed problems.* W. H. Winston and Sons.

Tompkins, M. J. (2005). The role of vertical anisotropy in interpreting marine controlled-source electromagnetic data. In *SEG technical program expanded.* Society of Exploration Geophysicists.